

Antibacterial Prenylated *p*-Hydroxybenzoic Acid Derivatives from *Oberonia myosurus* and Identification of Putative Prenyltransferases

Fu-Cai Ren, Li Liu, Yong-Feng Lv, Xue Bai, Qian-Jin Kang, Xiao-Jing Hu, Hong-Dan Zhuang, Liu Yang, Jiang-Miao Hu,* and Jun Zhou*



Cite This: *J. Nat. Prod.* 2021, 84, 417–426



Read Online

ACCESS |



Metrics & More

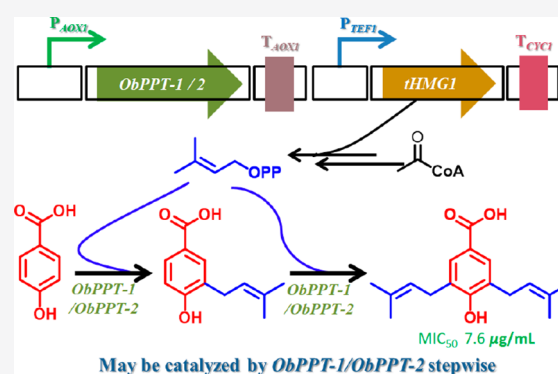


Article Recommendations



Supporting Information

ABSTRACT: Twelve hitherto unknown tandem prenylated *p*-hydroxybenzoic acid derivatives, namely, oberoniamyosurusins A–L, together with five known derivatives, were isolated from an EtOH extract of the whole parts of the plant *Oberonia myosurus*. Compounds **10**, **13**, and **17** exhibited moderate inhibitory activity against *Staphylococcus aureus* subsp. *aureus* ATCC29213 with MIC₅₀ values ranging from 7.6 to 23 μg/mL. To determine the biosynthetic pathway of this class of tandem prenyl-substituted compounds, the full-length transcriptome of *O. myosurus* was sequenced, yielding 19.09 Gb of clean data and 10 949 nonredundant sequences. Two isoforms of *p*-hydroxybenzoic acid prenyltransferases were annotated and functionally characterized as the enzymes that might be involved in the biosynthesis of nervogenic acid (**13**) in *Pichia pastoris*.



Prenylation is a major contributor to the diversity of natural products because of differences in prenylation position, various lengths of prenyl chain, and further modifications of the prenyl moiety.^{1,2} Prenylated aromatic compounds are hybrid natural products containing isoprenoid moieties or structures derived therefrom, and they display extensive structural diversity with various biological activities. The improvement of the lipophilicity and/or binding to the target protein by prenylation might be one of the causes of enhanced biological activities.³ Aromatic prenyltransferases catalyze the transfer of prenyl moieties to aromatic acceptor molecules and give rise to an astounding diversity of primary and secondary metabolites.⁴ A group of prenyltransferases can catalyze the transfer of allylic prenyl moieties to aromatic acceptor molecules, forming C–C bonds between C-1 or C-3 of the isoprenoid substrate and one of the aromatic carbons of the acceptor substrate, and they were found to carry out aromatic prenylations with different substrate, specificities, and regiospecificities and to catalyze both regular and reverse prenylations.^{4,5} In particular, prenylated *p*-hydroxybenzoic acid derivatives are a class of aromatic compounds that exhibit antimicrobial,⁶ anti-inflammatory,⁷ antiparasitic,⁸ and molluscicidal⁶ activities.

The genus *Oberonia* includes approximately 300 species of perennial herbs belonging to the plant family Orchidaceae.⁹ *Oberonia myosurus* Lindl. is used as a folk medicine by some ethnic minorities in southwestern China for the treatment of pneumonia, bronchitis, hepatitis, and urinary tract infections and externally for rheumatic bone pain. Nevertheless, studies on this plant are limited. In the course of our continual

research on chemical constituents from natural sources with pharmacological applications, phytochemical investigation of whole plants of *O. myosurus* led to the isolation of 17 prenylated *p*-hydroxybenzoic acid derivatives, including 12 new derivatives (**1**–**12**). All isolated compounds were evaluated for their potential antibacterial activity against four bacterial strains. ObPPT-1/ObPPT-2 were annotated from the full-length transcriptome of *O. myosurus* and functionally characterized as the enzymes that might be involved in the biosynthesis of nervogenic acid (**13**) in *Pichia pastoris*. Details of these efforts will be described below.

RESULTS AND DISCUSSION

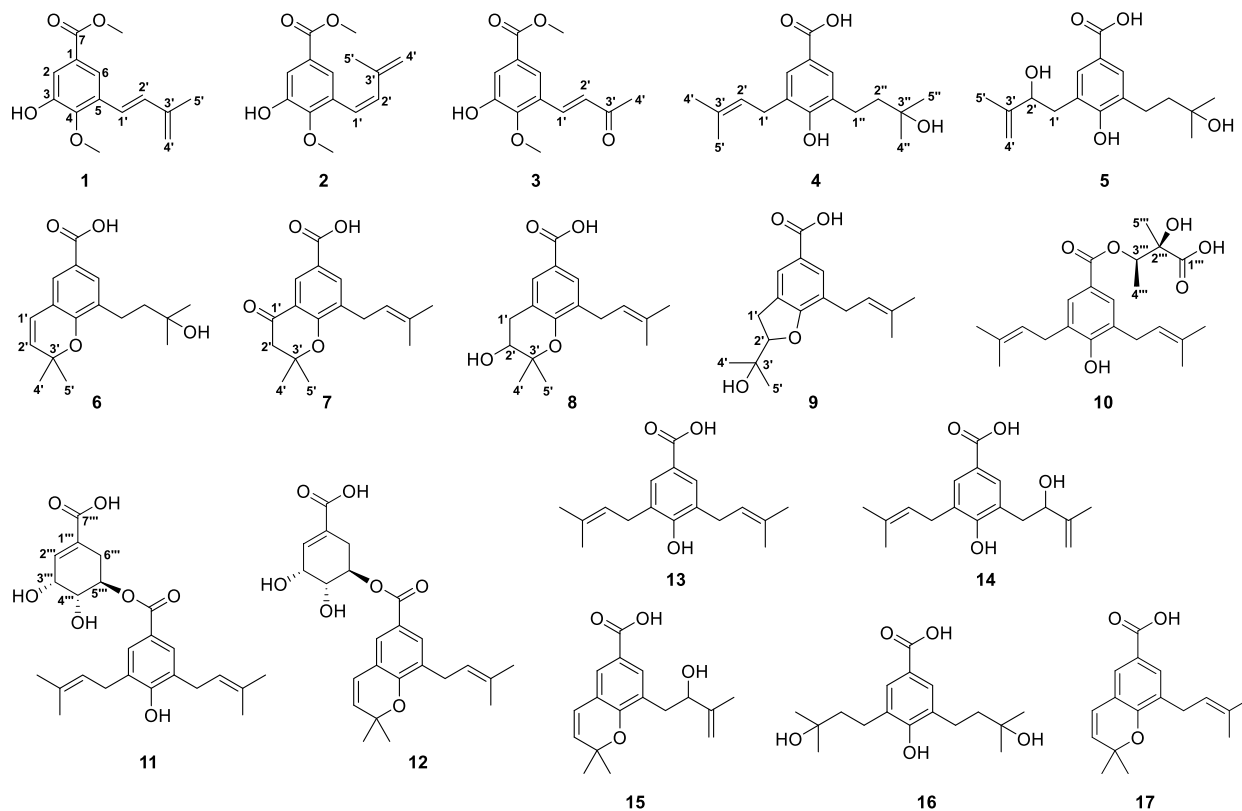
Compound **1** was isolated as a colorless oil. The IR spectrum indicated the presence of hydroxy (3407 cm^{−1}) and carbonyl (1719 cm^{−1}) groups and an aromatic ring (1591 and 771 cm^{−1}). The ¹H NMR spectrum (Table 1) displayed two meta-coupled aromatic doublets at δ_H 7.51 (1H, d, *J* = 2.0 Hz) and 7.79 (1H, d, *J* = 2.0 Hz), a pair of vinyl protons at δ_H 6.69 (1H, d, *J* = 16.2 Hz) and 6.98 (1H, d, *J* = 16.2 Hz), an exomethylene at δ_H 5.15 and 5.20 (each, 1H, s), a methyl singlet at δ_H 2.00 (3H, s), and two methoxy groups at δ_H 3.84 and

Received: October 13, 2020

Published: January 25, 2021



Chart 1

Table 1. ^1H and ^{13}C NMR Spectroscopic Data for Compounds 1–3^a

no.	1		2		3	
	δ_{C} , type ^b	δ_{H} , m, J (Hz) ^c	δ_{C} , type ^d	δ_{H} , m, J (Hz) ^e	δ_{C} , type ^f	δ_{H} , m, J (Hz) ^e
1	126.7, C		125.5, C		127.0, C	
2	115.3, CH	7.51, d (2.0)	115.1, CH	7.52, d (2.0)	118.5, CH	7.65, d (2.0)
3	148.9, C		148.2, C		149.3, C	
4	148.3, C		148.4, C		150.0, C	
5	130.7, C		130.4, C		127.9, C	
6	119.9, CH	7.79, d (2.0)	124.3, CH	7.48, d (2.0)	121.1, CH	7.84, d (2.0)
7	166.6, C		166.8, C			
1'	121.7, CH	6.69, d (16.2)	123.6, CH	6.43, d (12.3)	136.4, CH	7.73, d (16.5)
2'	134.5, CH	6.98, d (16.2)	134.9, CH	6.32, d (12.3)	129.2, CH	6.85, d (16.5)
3'	141.9, C		141.5, C		198.2, C	
4'	118.8, CH ₂	5.15, s	119.0, CH ₂	5.02, s	28.0, CH ₃	2.41, s
		5.20, s		5.02, s		
5'	18.5, CH ₃	2.00, s	21.6, CH ₃	1.66, s		
COOCH ₃	52.2, CH ₃	3.90, s	52.1, CH ₃	3.88, s	52.4, CH ₃	3.91, s
OCH ₃ -4	61.7, CH ₃	3.84, s	61.1, CH ₃	3.88, s	62.4, CH ₃	3.88, s

^aMeasured in CDCl₃ (δ_{H} 7.26 ppm, δ_{C} 77.0 ppm). ^bRecorded at 125 MHz. ^cRecorded at 500 MHz. ^dRecorded at 150 MHz. ^eRecorded at 600 MHz. ^fRecorded at 100 MHz.

3.90 (each, 3H, s). The ^{13}C and DEPT spectra showed a total of 14 carbon resonances including an aromatic ring [δ_{C} 126.7 (s, C-1), 115.3 (d, C-2), 148.9 (s, C-3), 148.3 (s, C-4), 130.7 (s, C-5), and 119.9 (d, C-6)], a carbonyl carbon (δ_{C} 166.3), an isoprene chain including a double bond (δ_{C} 121.7, 134.5) and an *exo*-methylene (δ_{C} 118.8), an ester methoxy group (δ_{C} 52.2), and an aromatic methoxy group (δ_{C} 61.7). Those mentioned NMR data together with the HMBC correlations (Figure S1) from the methoxy group at δ_{H} 3.84 (3H, s) to C-4, from H-1' to C-4, C-5, C-6, and C-3', from H-2' to C-5 and C-4', and from H-4' to C-2', C-3', and C-5' revealed that

compound 1 was a 3,4,5-trisubstituted benzoic acid methyl ester derivative with a hydroxy group, a methoxy group, and a "3-methyl-1,3-butadienyl" moiety located at C-3, C-4, and C-5, respectively. The diagnostic coupling constant ($J = 16.2$ Hz) between H-1' and H-2' suggested C-1' = C-2' was an *E*-form olefin. Therefore, the structure of compound 1 was established as (*E*)-3-hydroxy-4-methoxy-5-(3-methyl-1,3-butadienyl)-benzoic acid methyl ester and named as oberoniamyosurusin A.

The NMR data of compound 2 (Table 1) were very similar to those of 1, except for the ^1H NMR data of H-1' and H-2'

and the diagnostic coupling constant ($J = 12.3$ Hz) between them which suggested a *Z*-form double bond of C-1' = C-2'. Then, the structure of compound 2 was established as (*Z*)-3-hydroxy-4-methoxy-5-(3-methyl-1,3-butadienyl)benzoic acid methyl ester and named as oberoniamyosurustin B.

Compound 3 was isolated as a colorless oil. The HRESIMS data indicated the molecular formula $C_{13}H_{14}O_5$. The 1D NMR spectra of 3 displayed a pair of aromatic doublets, two methoxy groups, a benzene ring, and a carboxylate, which indicated that 3 had a similar structure to oberoniamyosurustin A (1). The main difference is only that 3 had a newly arising keto carbon at δ_C 198.2 instead of the terminal olefin. Thus, compound 3 might be the oxidation derivative of 1. And this was confirmed by the HMBC correlations from H-1' (δ_H 7.73) to C-4, C-5, C-6, and C-3', from H-2' (δ_H 6.85) to C-5 and C-4', and from H-4' to C-2' and C-3'. Hence, compound 3 was assigned as (*E*)-3-hydroxy-4-methoxy-5-(3-oxo-1,3-butadienyl)benzoic acid methyl ester and named as oberoniamyosurustin C.

Table 2. 1H NMR Spectroscopic Data for Compounds 4–9

no.	4 ^a	5 ^a	6 ^a	7 ^b	8 ^b	9 ^b
2	7.75, s (2.2)	7.68, d (2.2)	7.61, d (2.2)	8.15, d (2.2)	7.48, s	7.56, s
6	7.75, s	7.78, d (2.2)	7.77, d (2.2)	7.90, d (2.2)	7.47, s	7.50, s
1'	3.38, d (7.2)	2.85, dd (14.8, 2.3)	6.34, d (9.9)		2.61, dd (16.6, 7.9)	3.14, d (8.7)
		2.98, dd (14.8, 8.9)			2.91, dd (16.6, 5.2)	
2'	5.33, t (7.2)	4.40, dd (8.9, 2.3)	5.64, d (9.9)	2.84, s	3.64, dd (7.9, 5.2)	4.60, t (8.7)
4'	1.77, s	4.88, s 5.00, s	1.45, s	1.40, s	1.28, s	1.12, s
5'	1.76, s	1.81, s	1.45, s	1.40, s	1.15, s	1.07, s
1''	2.75, t (7.3)	2.75, m	2.68, m	3.29, d (7.4)	3.18, d (7.4)	3.20, d (7.3)
2''	1.80, t (7.3)	1.79, t (7.6)	1.75, m	5.14, t (7.4)	5.20, t (7.4)	5.23, t (7.3)
4''	1.31, s	1.29, s	1.31, s	1.69, s	1.67, s	1.66, s
5''	1.31, s	1.29, s	1.31, s	1.69, s	1.67, s	1.65, s

^aMeasured in $CDCl_3$ (δ_H 7.26 ppm). ^bMeasured in $DMSO-d_6$ (δ_H 2.49 ppm). Recorded at 600 MHz.

The 1H and ^{13}C NMR spectra (Tables 2 and 3) of compound 4, a light yellow oil, exhibited a set of signals at δ_H 7.75 (2H, s), δ_C 120.7, 130.5, 128.7, 157.6, 127.9, and 131.2, characteristic of a 1,3,4,5-tetrasubstituted aromatic ring, a carbonyl resonance at δ_C 172.0, and a prenyl group at δ_H 3.38 (2H, d, $J = 7.2$ Hz), 5.33 (1H, t, $J = 7.2$ Hz), 1.76 (3H, s), 1.77 (3H, s), δ_C 29.3, 121.6, 134.5, 25.8, and 17.9. The remaining signals at δ_H 1.80 (2H, t, $J = 7.3$ Hz, H-2''), 2.75 (2H, t, $J = 7.3$ Hz, H-1''), 1.31 (6H, s, H-4'' and H-5''), δ_C 24.7, 42.7, 71.9, 29.4, and 29.4 were assigned as a 3-hydroxy-3-methylbutyl moiety. The moiety was located at C-5 according to the HMBC correlations from H-1'' to C-4, C-5, and C-6, from H-2'' to C-5, and from H-4'' (H-5'') to C-2'' and C-3''. Then, compound 4 was established as 4-hydroxy-3-prenyl-5-(3-hydroxy-3-methylbutyl)benzoic acid, which biologically derives from nervogenic acid (13),⁶ and was given the trivial name oberoniamyosurustin D.

The NMR spectra of compounds 5 and 6 showed a 3,4,5-trisubstituted benzoic acid skeleton and a 3-hydroxy-3-methylbutyl side chain at C-5 relating as in compound 4. For compound 5, the remaining signals [δ_H 2.85 (1H, dd, $J = 14.8, 2.3$ Hz, H-1'), 2.98 (1H, dd, $J = 14.8, 8.9$ Hz, H-1'), 4.40 (1H, dd, $J = 8.9, 2.3$ Hz, H-2'), 4.88, 5.00 (each 1H, s, H-4'), 1.81 (3H, s, H-5'); δ_C 38.1, 77.8, 146.3, 111.3, 18.2] were due to a 2-hydroxy-3-methylbut-3-en-1-yl unit, which was confirmed by the HMBC correlations from H-2' to C-1', C-3', and C-4' and from H-5' to C-2', C-3', and C-4'. This moiety was assigned to C-3 according to the HMBC correlations from H-1' to C-2, C-3, and C-4 and from H-2' to C-3. The small rotation value and chiral-phase analysis suggested that compound 5 is racemic. For compound 6, the remaining protons at δ_H 5.64, 6.34 (each 1H, dd, $J = 9.9$ Hz) and 1.45 (6H, s) are typical for a fused 2,2-dimethylpyran ring being attached to the C-3 and C-4 oxygen of the aromatic ring. Hence, compounds 5 and 6 were established and named as oberoniamyosurustins E and F, respectively.

Compound 7 was isolated as a colorless oil. The 1H NMR spectrum revealed the presence of two *meta*-coupled aromatic doublets at δ_H 7.90 and 8.15 (each, 1H, d, $J = 2.2$ Hz) and a prenyl group similar to nervogenic acid, except for the replacement of one prenyl group with a prenyl-derived unit. The signals at δ_H 2.84 (2H, s), 1.40 (6H, s), and δ_C 191.9 indicated a 2,2-dimethyldihydropyran ring unit bearing a keto group at C-1', which was further confirmed from HMBC correlations from H-2' to C-1' and C-3 and from H-3'-4'(5') to C-2' and C-3'. This ring fused with the aromatic ring via the C-3 and C-4 oxygen was determined by the HMBC correlations from H-2 (δ_H 8.15) to C-1' and from H-2' (δ_H 2.84) to C-3 and C-3'. Therefore, compound 7 was established and named as oberoniamyosurustin G.

The NMR data of compounds 8 and 9 were similar to those of compound 7 except for the isoprenoid ring. For compound 8, a 2,2-dimethyl-3-hydroxydihydropyran ring was assigned according to the typical signals at δ_H 1.15, 1.28 (each, 3H, s), 2.61 (1H, dd, $J = 16.6, 7.9$ Hz), 2.91 (1H, dd, $J = 16.6, 5.2$ Hz), and 3.64 (1H, dd, $J = 7.9, 5.2$ Hz). For compound 9, the characteristic protons at δ_H 3.14 (2H, d, $J = 8.7$ Hz), 4.60 (1H, t, $J = 8.7$ Hz), and 1.07, 1.12 (each 3H, s) due to a 2-(1-hydroxy-1-methylethyl)-2,3-dihydrobenzofuran moiety were obviously distinguished. The chiral-phase analysis as well as the small rotation values implied that 8 and 9 were racemic. Hence, the structures of compounds 8 and 9 were established and named as oberoniamyosurustins H and I, respectively.

The NMR data of compound 10 (Table 4) showed it was a nervogenic acid (13) ester. The esterification group was established as a 2,3-dihydroxy-2-methylbutyryloxy unit according to the HMBC correlations from H-4''' (δ_H 1.36, d, $J = 6.4$ Hz) to C-3''' (δ_C 74.5) and C-2''' (δ_C 76.3) and from H-5''' (δ_H 1.42, s) to C-1''' (δ_C 178.7), C-2'', and C-3'''. The chemical shift of H-3''' (δ_H 5.25) indicated that the hydroxy group at C-3''' was esterified, which was further confirmed by the HMBC correlation from H-3''' to C-7 (δ_C 165.8). The ECD calculations suggested that 10b matched well with the experimental data of 10 (Figure 1), revealing the absolute configuration to be the *R,R*-form. Compound 10 was established and named as oberoniamyosurustin J.

The NMR data of compound 11 showed the presence of a nervogenic acid (13) moiety, and the remaining signals [δ_H 2.21, br dd, ($J = 18.3, 6.1$ Hz), 2.62, br. dd, ($J = 18.3, 4.4$ Hz)/ δ_C 27.1; δ_H 3.80, dd, ($J = 6.1, 4.4$ Hz)/ δ_C 67.3; δ_H 5.16, dt, ($J =$

Table 3. ^{13}C NMR Spectroscopic Data for Compounds 4–9

no.	4 ^{a,c}	5 ^{a,d}	6 ^{a,c}	7 ^{b,d}	8 ^{b,d}	9 ^{b,d}
1	120.7, C	120.6, C	121.5, C	123.1, C	124.7, C	122.7, C
2	130.5, CH	131.8, CH	126.7, CH	125.5, CH	129.2, CH	124.2, CH
3	128.7, C	125.6, C	120.4, C	119.2, C	119.5, C	127.7, C
4	157.6, C	158.8, C	155.3, C	160.3, C	153.4, C	161.9, C
5	127.9, C	130.5, C	129.9, C	131.1, C	128.0, C	122.0, C
6	130.3, CH	131.2, CH	131.9, CH	135.7, CH	128.3, CH	130.0, CH
7	172.0, C	171.1, C	171.5, C	166.7, C	168.4, C	167.7, C
1'	29.3, CH ₂	38.1, CH ₂	122.0, CH	191.9, C	31.1, CH ₂	29.7, CH ₂
2'	121.6, CH	77.8, CH	130.6, CH	47.5, CH ₂	67.8, CH	90.0, CH
3'	134.5, C	146.3, C	77.4, C	80.2, C	77.7, C	70.5, C
4'	25.8, CH ₃	111.3, CH ₂	28.4, CH ₃	26.1, CH ₃	25.8, CH ₃	26.2, CH ₃
5'	17.9, CH ₃	18.2, CH ₃	28.4, CH ₃	26.1, CH ₃	20.7, CH ₃	24.5, CH ₃
1''	24.7, CH ₂	25.2, CH ₂	24.6, CH ₂	27.8, CH ₂	28.1, CH ₂	27.9, CH ₂
2''	42.7, CH ₂	43.4, CH ₂	43.7, CH ₂	121.4, CH	122.6, CH	121.8, CH
3''	71.9, C	71.5, C	71.2, C	132.6, C	131.3, C	132.5, C
4''	29.4, CH ₃	29.2, CH ₃	29.1, CH ₃	25.6, CH ₃	25.6, CH ₃	25.8, CH ₃
5''	29.4, CH ₃	29.2, CH ₃	29.1, CH ₃	17.8, CH ₃	17.7, CH ₃	17.9, CH ₃

^aMeasured in CDCl₃ (δ_{C} 77.0 ppm). ^bMeasured in DMSO-*d*₆ (δ_{C} 39.5 ppm). ^cRecorded at 100 MHz. ^dRecorded at 150 MHz.

Table 4. ^1H and ^{13}C NMR Spectroscopic Data for Compounds 10–12

no.	10 ^a		11 ^b		12 ^a	
	δ_{C} , type ^c	δ_{H} , m, J (Hz) ^d	δ_{C} , type ^c	δ_{H} , m, J (Hz) ^d	δ_{C} , type ^c	δ_{H} , m, J (Hz) ^d
1	121.5, C		120.5, C		121.2, C	
2	129.8, CH	7.60, s	128.1, CH	7.47, s	126.2, CH	7.43, s
3	127.0, C		128.5, C		120.4, C	
4	157.4, C		157.1, C		155.2, C	
5	127.0, C		128.5, C		129.3, C	
6	129.8, CH	7.60, s	128.1, CH	7.47, s	131.4, CH	7.59, s
7	165.8, C		162.2, C		166.5, C	
1'	29.4, CH ₂	3.30, d (7.4)	28.0, CH ₂	3.27, d (7.4)	28.3, CH ₂	3.21, d (6.8)
2'	121.2, CH	5.25, overlapped	122.0, CH	5.24, t (7.4)	122.0, CH	5.19, t (6.8)
3'	134.9, C		132.4, C		132.3, C	
4'	25.7, CH ₃	1.76, s	25.5, CH ₃	1.70, s	25.7, CH ₃	1.67, s
5'	17.8, CH ₃	1.74, s	17.7, CH ₃	1.64, s	17.9, CH ₃	1.68, s
1''	29.4, CH ₂	3.30, d (7.4)	28.0, CH ₂	3.27, d (7.4)	122.1, CH	6.27, d (9.8)
2''	121.2, CH	5.25, overlapped	122.0, CH	5.24, t (7.4)	130.6, CH	5.57, d (9.8)
3''	134.9, C		132.4, C		77.2, C	
4''	25.7, CH ₃	1.76, s	25.5, CH ₃	1.70, s	28.2, CH ₃	1.38, s
5''	17.8, CH ₃	1.74, s	17.7, CH ₃	1.64, s	28.2, CH ₃	1.38, s
1'''	178.7, C		127.9, C		129.6, C	
2'''	76.3, C		138.7, CH	6.68, br s	137.8, CH	6.92, br s
3'''	74.5, CH	5.25, overlapped	65.6, CH	4.25, br s	66.4, CH	4.53, br s
4'''	13.4, CH ₃	1.36, d (6.4)	67.3, CH	3.80, dd, (6.1, 4.4)	69.1, CH	4.03, br s
5'''	21.6, CH ₃	1.42, s	70.2, CH	5.16, dt, (6.1, 4.4)	70.0, CH	5.39, t (6.9)
6'''			27.1, CH ₂	2.21, br dd (18.3, 6.1), 2.62, dd (18.3, 4.4)	27.8, CH ₂	2.40, br d (16.1) 2.87, br d, (16.1)
7'''			170.2, C		170.2, C	

^aMeasured in CDCl₃ (δ_{H} 7.26 ppm, δ_{C} 77.0 ppm). ^bMeasured in DMSO-*d*₆ (δ_{H} 2.49 ppm, δ_{C} 39.5 ppm). ^cRecorded at 150 MHz. ^dRecorded at 600 MHz.

6.1, 4.4 Hz)/ δ_{C} 70.2; δ_{H} 6.68 (br s); δ_{C} 127.9, 170.2] could be recognized as a shikimic acid ester.¹⁰ The esterification of the C-5''' hydroxy group and the C-7 carboxyl of nervogenic acid (13) could be confirmed by the chemical shift of H-5''' (δ_{H} 5.16) and the HMBC correlation from H-5''' to C-7. The NMR data of compound 12 indicated that 12 possesses a similar structure to a shikimic acid ester moiety, except the 2,2-dimethyl-8-prenylchromene-6-carboxylic acid (17) moiety replaced the nervogenic acid (13) in compound 11. The absolute configurations of compounds 11 and 12 were

postulated as *R,R,R*-form in light of a negative specific rotation value (−89.6, −93.1, MeOH), consistent with that of (*R,R,R*)-3-*O*-galloylshikimic acid (−108.3, MeOH).¹¹ Hence, compounds 11 and 12 were established and named as oberoniamyosurusins K and L, respectively.

In addition, except for the new substances described above, five known prenylated *p*-hydroxybenzoic acid derivatives were also isolated from *O. myosurus*, which were identified as nervogenic acid (13),⁶ (4-hydroxy-3-(2-hydroxy-3-methyl-3-butenyl)-5-(3-methyl-2-butenyl)benzoic acid (14),⁸ liparacids

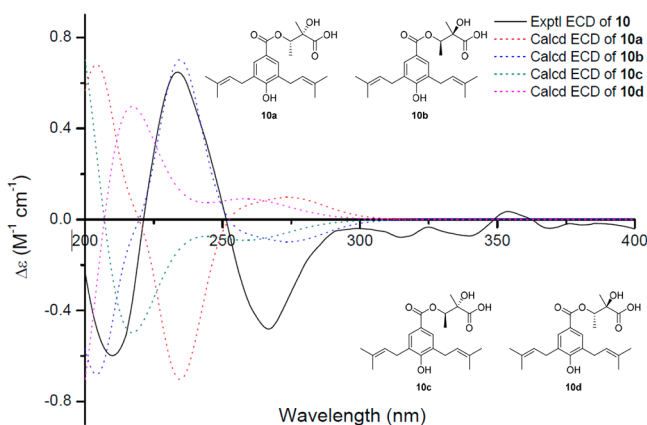


Figure 1. ECD calculations for 10.

A and C (15, 16),¹² and 2,2-dimethyl-8-prenylchromene-6-carboxylic acid (17)¹³ by comparing their NMR data with literature values.

In accordance with the background of folk medicine application of *O. myosurus*, all isolated compounds were evaluated for their potential antibacterial activity against the four bacterial strains *Escherichia coli* ATCC25922, *Staphylococcus aureus* subsp. *aureus* ATCC29213, *Salmonella enterica* subsp. *enterica* ATCC14028, and *Pseudomonas aeruginosa* ATCC27853. Ceftazidime and penicillin G sodium salt were used as positive controls. Some isolates exhibited inhibitory activity against *Staphylococcus aureus* subsp. *aureus* ATCC29213. Compounds 10, 13, and 17 exhibited moderate inhibitory activity with MIC₅₀ values ranging from 7.6 to 23 μg/mL, whereas compounds 7, 12, 14, and 15 exhibited modest inhibitory potency with MIC₅₀ values ranging from 56 to 93 μg/mL (Table 5).

Table 5. MIC₅₀ Values of Compounds 7, 10, 12, 13, 14, 15, and 17 against *Staphylococcus aureus* subsp. *aureus* ATCC29213

sample	MIC ₅₀ (μg/mL)
penicillin G sodium salt	0.53 ± 0.03
compd 7	93 ± 2
compd 10	23 ± 1
compd 12	56 ± 1
compd 13	7.6 ± 1.0
compd 14	89 ± 1
compd 15	81 ± 5
compd 17	15 ± 1

All of the isolated compounds exhibited one or two prenyl groups (cyclization and hydroxylation included) at C-3 or C-5, and most of those could be obtained from nervogenic acid (13) through enzymatic or nonenzymatic reactions (Scheme 1). Specifically, nervogenic acid (13) is a diprenyl-substituted compound and could be directly biosynthesized from *p*-hydroxybenzoic acid (PHB) and dimethylallyl diphosphate (DMAPP).^{5,14} DMAPP is an important intermediate in the biosynthesis of terpenes, whereas PHB can be obtained through the shikimic acid pathway via chorismic acid as the last intermediate.¹⁵

To gain insight into the biosynthetic pathway of this class of tandem prenyl-substituted compounds, the full-length transcriptome of *O. myosurus* was sequenced, yielding 19.09 Gb of

clean data and 207 191 circular consensus (CCS) reads, including 165 339 full-length nonchimeric (FLNC) sequences. By clustering FLNC sequences and performing polishing, 19 451 high-quality consensus sequences were obtained. Then, 10 949 nonredundant transcript sequences were captured, and 10 181 sequences were subjected to functional annotations blasting with the NR, SwissProt, GO, COG, KOG, Pfam, and KEGG databases. Subsequently, two unique isoforms (*ObPPT-1* and *ObPPT-2*) were annotated as encoding 4-hydroxybenzoate polyprenyltransferase enzymes.

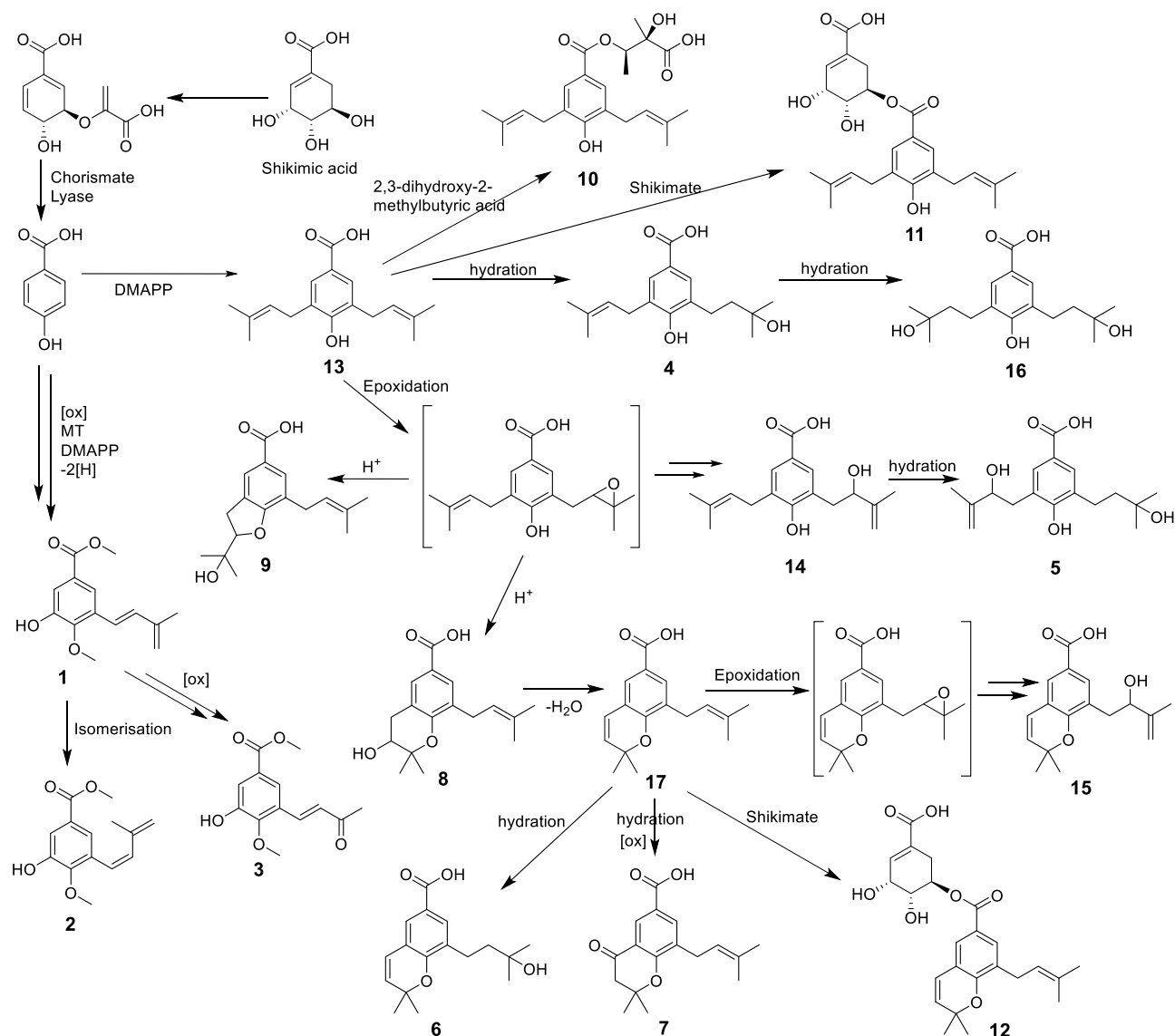
Molecular phylogenetic analysis showed that the *ObPPT-1* and *ObPPT-2* formed a new sub-branch of prenyltransferases in ubiquinone biosynthesis (Figure 2). Multiple sequence alignments with plant aromatic prenyltransferases with known functions showed that the protein sequence of *ObPPT-1/ObPPT-2* shared approximately 52% identity with *AtPPT1*, which catalyzes isoprenylation with solanesyl diphosphate to produce 3-solanesyl-4-hydroxybenzoate,¹⁶ and shared only 28.5% identity with *XimB*, which utilizes GPP as a substrate (Figure S2).¹⁷ Sequence alignment showed that a putative prenyl diphosphate binding site consisting of NDXXD and the GXKSTAL motif was present in *ObPPT-1* and *ObPPT-2*.¹⁴ The TMHMM 2.0 online analysis tool was used to predict the transmembrane area of *ObPPT-1/ObPPT-2* and clearly showed that *ObPPT-1/ObPPT-2* has six transmembrane areas (Figure 3). Because eukaryotic expression systems have many advantages over prokaryotic expression systems for the heterologous expression of membrane proteins,¹⁸ the *Pichia pastoris* expression system with a substrate incubation method was chosen to investigate the functions of *ObPPT-1/ObPPT-2*.

To analyze the functions of these two isoforms of putative 4-hydroxybenzoate polyprenyltransferases, genetic approaches were employed to create a DMAPP overproduction platform in *P. pastoris* to efficiently identify the functions of *ObPPT-1/ObPPT-2*. 3-Hydroxy-3-methylglutaryl-CoA (HMG-CoA) reductase is generally considered as the rate-limiting enzyme in the MVA pathway, and overexpression of a truncated HMG-CoA reductase gene (*tHMG1*) has commonly been used to increase the production of many terpenoids.^{19,20} The codon-optimized *ObPPT-1/ObPPT-2* gene (controlled by the AOX1 promoter) and the *tHMG1* gene (controlled by the TEF1 promoter) were integrated into the expression vector pPICZB (Invitrogen). The *P. pastoris* yeast strain SMD1168H was transformed using electroporation.

SMD1168Hs harboring the *ObPPT-1/ObPPT-2* and *tHMG1* genes were grown in BMMY medium with PHB as the supplemented precursor and induced with 0.5% MeOH for 120 h. As a result, two newly appearing ion peaks were detected using GC-MS in the supernatant of the fermentation broth compared with the control strain without the *ObPPT-1/ObPPT-2* gene inserted (Figures 4, S3). The fragment ion peak with a retention time of 18.2 min occurring at *m/z* 162 led us to speculate that this might be a decarboxylated fragment of 4-hydroxy-3-prenylbenzoic acid, which was caused by heating. To verify this inference and determine whether the *ObPPT-1/ObPPT-2* gene has the biological function of catalyzing the second prenyl group, 4-hydroxy-3-prenylbenzoic acid was chemically synthesized from 4-hydroxybenzoic acid with a total yield of 43% through a three-step reaction (Scheme 2).²¹

Subsequently, the above deduction was confirmed in view of the consistency between the supernatant of the fermentation broth extract and the chemically synthesized standard specimen using GC-MS (Figures 4, S3, S4). In addition, 4-

Scheme 1. Proposed Routes of Formation of Compounds Isolated from *Oberonia myosurus*



hydroxy-3-prenylbenzoic acid was also used as a precursor substrate for the fermentation. Subsequently, two significant peaks both occurring at m/z 230 (decarboxylated fragments) were detected using GC-MS in the supernatant of the fermentation broth, and the peak at 25.0 min was recognized as nervogenic acid (**13**) by comparison with the naturally separated standard (Figures 4, S5). Regrettably, the structure of the peak of 24.0 has not yet been determined, but it is clear that it is not the product of an *O*-prenylated product (compound **22** in the Supporting Information) by GC-MS. Therefore, *ObPPT-1/ObPPT-2* can produce low levels of the prenylated PHB products and the enzymes might be involved in the biosynthesis of nervogenic acid (**13**).

In summary, phytochemical investigation of whole plants of *O. myosurus* supported the chemical basis of its traditional medicine applications and provides a new idea for the discovery of plant-derived antibiotics. With the help of genetic engineering, we identified *ObPPT-1* and *ObPPT-2*, two isoforms of 4-hydroxybenzoate prenyltransferase that may be involved in the prenylation of PHB from *O. myosurus*. Our study provides an approach to the functional and mechanistic

characterization of prenyltransferases using the DMAPP overproduction platform in *P. pastoris*, and this approach might be further extended to other prenyltransferases of various origins. This may speed up the process of discovering new prenyltransferases and prenylated compounds with high value added or various biological activities for drug discovery or industrial applications.

■ EXPERIMENTAL SECTION

General Experimental Procedures. Optical rotations were measured in MeOH with Horiba SEPA-300 and JASCO P-1020 polarimeters. UV spectra were recorded on a Shimadzu UV-2700 spectrophotometer. ECD were obtained on an Applied Photophysics Chirascan apparatus. IR spectra (KBr) were obtained on a Bruker Tensor-27 infrared spectrophotometer. NMR spectra were carried out on Bruker Avance III 600, Bruker DRX-500, or Bruker Avance III 400 spectrometers with deuterated solvent signals used as internal standards. ESIMS and HRESIMS were collected on an Agilent G6230 time-of-flight or an Agilent 1290 UPLC/6540 Q-TOF mass spectrometer. Column chromatography (CC) was performed on silica gel (100–200 and 200–300 mesh, Qingdao Haiyang Chemical Co., Ltd.), Lichroprep RP-18 (43–63 μm , Merck), YMC*-GEL ODS-A (12 nm, S-50 μm , YMC), MCI gel (CHP20P, 75–150 μm , Mitsubishi

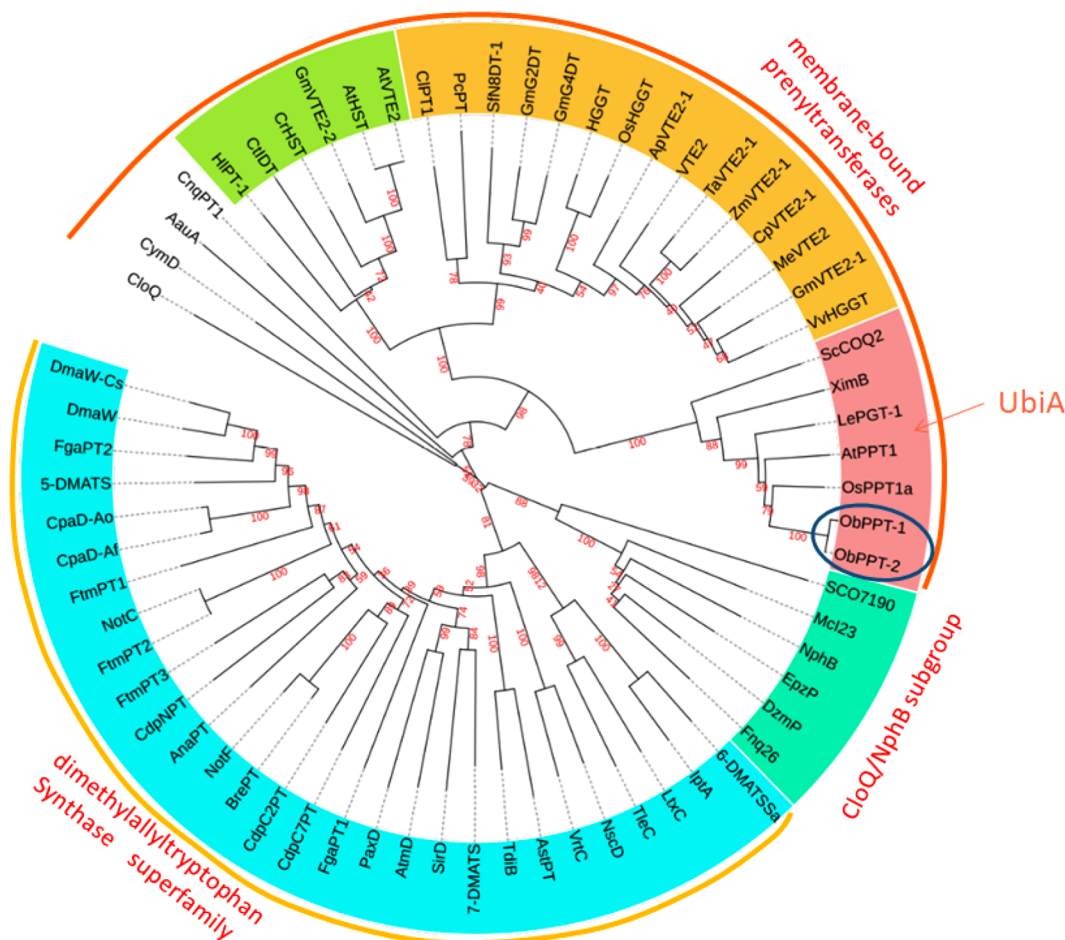


Figure 2. Phylogenetic analysis of *ObPPT-1*, *ObPPT-2*, and other aromatic prenyltransferases. The sequence information on aromatic prenyltransferases is listed in Table S3. Branches are labeled with the percentage based on 1000 bootstrap replicates.

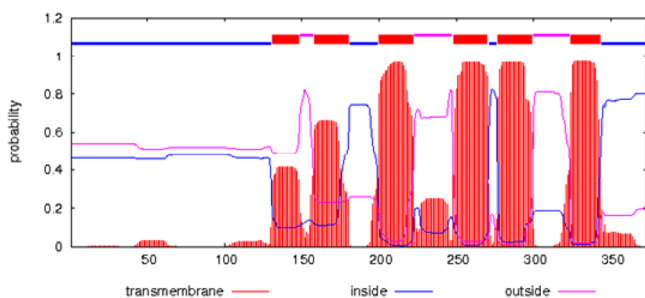


Figure 3. Predictive analysis of the transmembrane section of *ObPPT-1* through the TMHMM 2.0 online analysis.

Chemical Corporation), and Sephadex LH-20 (Amersham Biosciences AB). Semipreparative HPLC was carried out on an Agilent 1100 HPLC with a Zorbax SB-C₁₈ (9.4 × 250 mm, Agilent) column. Fractions were monitored by TLC plates (Si gel G and GF₂₅₄, Qingdao Haiyang Chemical Co., Ltd.), and spots were visualized by heating silica gel plates sprayed with 10% H₂SO₄ in EtOH.

Plant Material. The whole plants of *Oberonia myosurus* were purchased from Wenshan Hengfeng farmers market, Wenshan Zhuang and Miao Autonomous Prefecture, Yunnan Province, People's Republic of China, in September 2017. The plant was identified by Dr. Ende Liu of Kunming Institute of Botany, Chinese Academy of Sciences. A voucher specimen (KIBZJ-20170901) was deposited at the State Key Laboratory of Phytochemistry and Plant Resources in West China, Kunming Institute of Botany, Chinese Academy of Sciences.

Extraction and Isolation. The whole herbs of *O. myosurus* (2.5 kg) were air-dried and powdered, then extracted three times with 95% EtOH (15 L × 3) at room temperature, and then filtered. The extracts were combined and concentrated to afford an organic extract (ca. 260 g), which was fractionated by silica gel CC and eluted successively with a gradient of increasing acetone in petroleum ether (50:1, 15:1, 10:1, 5:1, 2:1, 1:1, 0:1; v/v) and then MeOH to afford fractions A–H, respectively. Fraction B was separated by Sephadex LH-20 (CHCl₃–MeOH, 1:1) and preparative thin layer chromatography (TLC) to yield compounds 1 (44 mg), 2 (17 mg), and 3 (8 mg). Fraction C was further purified by passage over repeated silica gel (CHCl₃–MeOH, 100:0 → 20:1) and Sephadex LH-20 (CHCl₃–MeOH, 1:1) CC to yield compounds 10 (490 mg), 13 (910 mg), and 17 (112 mg). Fraction D was separated sequentially using silica gel (CHCl₃–MeOH, 100:0 → 10:1), MCI resin (MeOH–H₂O, 100:0 → 4:1), and Sephadex LH-20 (MeOH) and then preparative HPLC to afford compounds 4 (97 mg), 6 (112 mg), 7 (12 mg), 8 (7 mg), 9 (9 mg), 14 (19 mg), and 15 (154 mg). Compounds 5 (136 mg) and 16 (257 mg) were isolated from fraction E using silica gel (CHCl₃–MeOH, 100:1 → 10:1), Sephadex LH-20 (MeOH), and RP-18 CC (MeOH–H₂O, 70%), respectively. Fraction F was purified by passage over repeated silica gel CC (CHCl₃–MeOH gradient, 50:1 → 5:1), followed by MCI resin (MeOH–H₂O, 40%), to yield compounds 11 (240 mg) and 12 (174 mg).

Oberoniamyosurusin A (1): colorless oil; UV (MeOH) λ_{\max} (log ϵ) 212 (4.29), 260 (4.57), 293 (4.31) nm; IR (KBr) ν_{\max} 3407, 2949, 2931, 1719, 1591, 1435, 1324, 1248, 1103, 1003, 911, 893, 771 cm^{−1}; ¹H and ¹³C NMR data, Table 1; HRESIMS m/z 271.0945 [M + Na]⁺ (calcd for C₁₄H₁₆O₄Na, 271.0941).

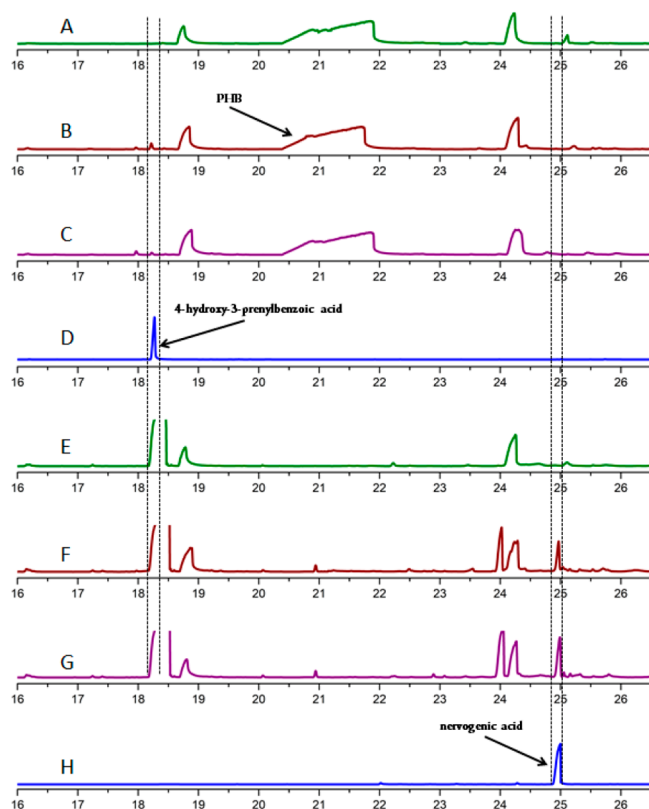
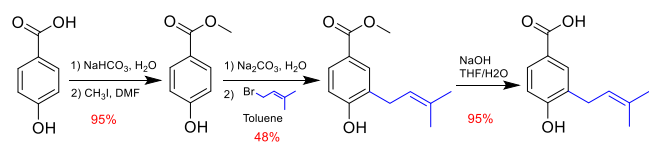


Figure 4. Total ion GC/MS chromatogram with PHB as the substrate: (A) SMD1168H:: P_{EFI} -tHMG1- T_{CYC1} ; (B) SMD1168H:: P_{AOX1} -ObPPT-1- T_{AOX1} - P_{TEF1} -tHMG1- T_{CYC1} ; (C) SMD1168H:: P_{AOX1} -ObPPT-2- T_{AOX1} - P_{TEF1} -tHMG1- T_{CYC1} ; (D) chemically synthesized standard 4-hydroxy-3-prenylbenzoic acid and with 4-hydroxy-3-prenylbenzoic acid as the substrate; (E) SMD1168H:: P_{EFI} -tHMG1- T_{CYC1} ; (F) SMD1168H:: P_{AOX1} -ObPPT-1- T_{AOX1} - P_{TEF1} -tHMG1- T_{CYC1} ; (G) SMD1168H:: P_{AOX1} -ObPPT-2- T_{AOX1} - P_{TEF1} -tHMG1- T_{CYC1} ; (H) naturally separated standard nervogenic acid.

Scheme 2. Synthetic Route to 4-Hydroxy-3-prenylbenzoic Acid



Oberoniamyosurustin B (2): colorless oil; UV (MeOH) λ_{max} (log ϵ) 213 (4.54), 254 (4.22), 307 (3.98) nm; IR (KBr) ν_{max} 3426, 2953, 2927, 1718, 1604, 1436, 1383, 1330, 1222, 1169, 1014, 894, 771 cm^{-1} ; 1H and ^{13}C NMR data, Table 1; HRESIMS m/z 247.0978 $[M - H]^-$ (calcd for $C_{14}H_{15}O_4$, 247.0976).

Oberoniamyosurustin C (3): colorless oil; UV (MeOH) λ_{max} (log ϵ) 209 (4.52), 247 (4.14), 307 (3.85) nm; IR (KBr) ν_{max} 3420, 2954, 1721, 1639, 1586, 1434, 1356, 1269, 1248, 1214, 1013, 985, 972, 760 cm^{-1} ; 1H and ^{13}C NMR data, Table 1; HRESIMS m/z 273.0736 $[M + Na]^+$ (calcd for $C_{13}H_{14}O_5Na$, 273.0733).

Oberoniamyosurustin D (4): light yellow oil; UV (MeOH) λ_{max} (log ϵ) 195 (4.54), 208 (4.49), 257 (4.05) nm; IR (KBr) ν_{max} 3413, 2972, 2932, 1686, 1605, 1436, 1196, 906, 776 cm^{-1} ; 1H and ^{13}C NMR data, Tables 2 and 3; HRESIMS m/z 315.1570 $[M + Na]^+$ (calcd for $C_{17}H_{24}O_4Na$, 315.1572).

Oberoniamyosurustin E (5): light yellow oil; $[\alpha]_D^{27}$ -1.2 (c 0.29, MeOH); UV (MeOH) λ_{max} (log ϵ) 196 (4.46), 207 (4.45), 258 (4.00) nm; IR (KBr) ν_{max} 3393, 2972, 1686, 1603, 1408, 1299, 1205, 1060, 904, 776 cm^{-1} ; 1H and ^{13}C NMR data, Tables 2

and 3; HRESIMS m/z 331.1518 $[M + Na]^+$ (calcd for $C_{17}H_{24}O_5Na$, 331.1521).

Oberoniamyosurustin F (6): yellow oil; UV (MeOH) λ_{max} (log ϵ) 195 (4.15), 240 (4.33), 275 (3.44) nm; IR (KBr) ν_{max} 3424, 2969, 2930, 1682, 1643, 1603, 1378, 1233, 1126, 958, 906, 779 cm^{-1} ; 1H and ^{13}C NMR data, Tables 2 and 3; HRESIMS m/z 313.1413 $[M + Na]^+$ (calcd for $C_{17}H_{22}O_4Na$, 313.1416).

Oberoniamyosurustin G (7): colorless oil; UV (MeOH) λ_{max} (log ϵ) 196 (4.34), 234 (4.41), 327 (3.41) nm; IR (KBr) ν_{max} 3427, 2978, 2926, 1698, 1678, 1606, 1441, 1387, 1280, 1239, 1201, 1176, 925, 776 cm^{-1} ; 1H and ^{13}C NMR data, Tables 2 and 3; HRESIMS m/z 311.1262 $[M + Na]^+$ (calcd for $C_{17}H_{20}O_4Na$, 311.1259).

Oberoniamyosurustin H (8): light yellow oil; $[\alpha]_D^{25}$ $+4.2$ (c 0.22, MeOH); UV (MeOH) λ_{max} (log ϵ) 212 (4.33), 262 (4.03) nm; IR (KBr) ν_{max} 3424, 2978, 2930, 1687, 1607, 1436, 1383, 1280, 1194, 1139, 1061, 950.9, 774 cm^{-1} ; 1H and ^{13}C NMR data, Tables 2 and 3; HRESIMS m/z 313.1410 $[M + Na]^+$ (calcd for $C_{17}H_{22}O_4Na$, 313.1410).

Oberoniamyosurustin I (9): light yellow oil; $[\alpha]_D^{25}$ -2.2 (c 0.21, MeOH); UV (MeOH) λ_{max} (log ϵ) 205 (4.20), 263 (3.92) nm; IR (KBr) ν_{max} 3424, 2977, 2931, 1687, 1383, 1282, 1188, 963, 909, 776 cm^{-1} ; 1H and ^{13}C NMR data, Tables 2 and 3; HRESIMS m/z 289.1445 $[M - H]^-$ (calcd for $C_{17}H_{21}O_4$, 289.1440).

Oberoniamyosurustin J (10): light yellow oil; $[\alpha]_D^{25}$ $+12.7$ (c 0.23, MeOH); UV (MeOH) λ_{max} (log ϵ) 196 (4.47), 212 (4.41), 262 (4.09) nm; IR (KBr) ν_{max} 3436, 2979, 2927, 1716, 1695, 1603, 1450, 1355, 1313, 1281, 1196, 1102, 1051, 771 cm^{-1} ; 1H and ^{13}C NMR data, Table 4; HRESIMS m/z 413.1932 $[M + Na]^+$ (calcd for $C_{22}H_{30}O_6Na$, 413.1935).

Oberoniamyosurustin K (11): light yellow oil; $[\alpha]_D^{25}$ -89.6 (c 1.4, MeOH); UV (MeOH) λ_{max} (log ϵ) 195 (4.56), 209 (4.51), 264 (4.12) nm; IR (KBr) ν_{max} 3420, 2974, 2916, 1698, 1604, 1437, 1229, 1104, 1207, 905, 770 cm^{-1} ; 1H and ^{13}C NMR data, Table 4; HRESIMS m/z 453.1884 $[M + Na]^+$ (calcd for $C_{24}H_{30}O_7Na$, 453.1884).

Oberoniamyosurustin L (12): light yellow oil; $[\alpha]_D^{25}$ -93.1 (c 0.41, MeOH); UV (MeOH) λ_{max} (log ϵ) 195 (4.55), 247 (4.49), 281 (3.74) nm; IR (KBr) ν_{max} 3410, 2976, 2924, 1701, 1652, 1390, 1312, 1285, 1197, 1105, 1028, 907, 804 cm^{-1} ; 1H and ^{13}C NMR data, Table 4; HRESIMS m/z 451.1728 $[M + Na]^+$ (calcd for $C_{24}H_{28}O_7Na$, 451.1727).

ECD Calculations. Conformational analysis was performed using the MMFF94 molecular mechanics force field. The molecules of 10a, 10b, 10c, and 10d showed 15, 15, 20, and 20 stable conformers within an energy window of 3.0 kcal/mol, respectively. All these conformers were further optimized by the DFT calculation at the B3LYP/6-311G(d,p) level by Gaussian 09. The ECD values were calculated using time-dependent density functional theory (TDDFT) at the B3LYP/6-311G(d,p) level in methanol. The ECD curves were drawn using the Origin Pro 9 program (OriginLab Corporation, Northampton, MA, USA).

In Vitro Antimicrobial Assays. All of the compounds 1–17 were tested for their potential antibacterial activity against the four bacterial strains *Escherichia coli* ATCC25922, *Staphylococcus aureus* subsp. *aureus* ATCC29213, *Salmonella enterica* subsp. *enterica* ATCC14028, and *Pseudomonas aeruginosa* ATCC27853 (China General Microbiological Culture Collection Center) at the single concentration of 128 $\mu g/mL$. The tested bacteria strains were cultured in Mueller Hinton broth (Guangdong Huankai Microbial Sci. & Tech. Co., Ltd.) at 37 $^{\circ}C$ overnight with shaking (200 rpm). Briefly, the assays were performed in 96-well plates containing the mid log phase culture (50 μL) and the tested compound (150 μL). The final concentrations of culture and compound were 5×10^5 CFU/mL and 128 $\mu g/mL$, respectively. Plates were incubated for 24 h; then the absorbances at 625 nm were measured to determine the inhibition. All assays were performed in triplicate. Ceftazidime (Shanghai Yuanye Bio-Technology Co., Ltd.) and penicillin G sodium salt (Biosharp) were used as the positive controls. Subsequently, MIC assays were carried out in 96-well plates with an initial bacterial inoculum of 5×10^5 CFU/mL. The tested compounds 7, 10, 12, 13, 14, 15, and 17 were dissolved in

DMSO and further serial 2-fold diluted in medium, giving a final different compound concentration of 8–128 $\mu\text{g/mL}$. Plates were incubated for 24 h; then the absorbance at 625 nm was measured. MIC value was calculated according to the Reed and Muench method.²²

Strains and Media. *Escherichia coli* strains were grown in low-salt LB broth or agar at 37 °C. *P. pastoris* yeast strains were cultivated in YPD medium, and for induced growth, in BMGY/BMMY medium. The primers used in this study are summarized in Table S1, and strains and plasmids are listed in Table S2.

Full-Length Transcriptome Sequences. RNA-seq and bioinformatics analyses were conducted by Biomarker Technologies Corporation. Total RNA was extracted from frozen fresh leaves following the Biomarker protocol. After the samples are qualified, total RNA was reverse transcribed into cDNA using a SMARTer PCR cDNA synthesis kit; then the full-length cDNA was amplified by PCR. Terminal repair was performed on the full length cDNA, which was then connected to the SMRT dumbbell connector. The library was obtained by digestion with exonuclease.

Raw reads were processed into error-corrected reads of inserts (ROIs) using the Iso-seq pipeline with minFullPass = 0 and minPredictedAccuracy = 0.90. Next, FLNC transcripts were determined by searching for the polyA tail signal and the 5' and 3' cDNA primers in ROIs. ICE (iterative clustering for error correction) was used to obtain consensus isoforms, and full-length consensus sequences from ICE were polished using Quiver. High-quality full-length transcripts were classified with the criteria postcorrection accuracy above 99%. Then, Iso-Seq high-quality full-length transcripts for removing redundancy using cd-hit (identity >0.99) were used.

The raw data were uploaded to the Sequence Read Archive (SRA) (<http://www.ncbi.nlm.nih.gov/>) with accession SRR12052857. The transcriptome assembly project was deposited at DDBJ/EMBL/GenBank under the accession GISE00000000.

Phylogenetic Analysis of Aromatic Prenyltransferases. Multiple sequence alignment of aromatic prenyltransferases was performed using clustalW. Evolutionary analyses were conducted in MEGA X. The evolutionary history was inferred using the neighbor-joining method.²³ The evolutionary distances were computed using the Poisson correction method and are in units of the number of amino acid substitutions per site. This analysis involved 67 amino acid sequences. All ambiguous positions were removed for each sequence pair (pairwise deletion option). There were a total of 579 positions in the final data set.

Construction of Plasmids and Mutants. The strain to express sufficient precursor DMAPP in *P. pastoris* was constructed according to the following procedure: *ObPPT-1* and *ObPPT-2* were made by synthesis, with yeast-preferred codons incorporated into the sequence, then introduced into the pUC57 vector (Genewiz). The plasmids were double-digested with *Xho*I and *Not*I and ligated into the yeast expression vector pPICZB to generate the plasmids pBOB01 and pBOB02, respectively. The *tHMG1* gene was PCR amplified from *Saccharomyces cerevisiae* S288C chromosomal DNA, using the primer pair P3/P4. The promoter P_{TEF1} and the T_{CYC1} terminator were amplified from pPICZB using primer pairs P1/P2 and P5/P6, respectively. Then, P_{TEF1} , *tHMG1*, and T_{CYC1} were assembled using splicing by overlap extension PCR (SOE-PCR) using the primer pair P1/P6. The amplified products were cloned into the pBluescript SK(+) vector and sequenced from both ends. Then, the plasmids were digested with *Bam*HI and inserted into same enzyme-digested pPICZB, pBOB01, and pBOB02 for the construction of plasmid pBOB03, pBOB04, and pBOB05, respectively. Plasmids pBOB03–05 was linearized with *Dra*I and inserted into the AOX1 site of *P. pastoris* yeast SMD1168H to generate the strains SOB03–05, respectively, using electroporation according to the protocol described in the EasySelect Pichia expression kit (Invitrogen).

Plasmid maps of pBOB03–05 were uploaded to Benchling and can be obtained through the Web site freely: <https://benchling.com/s/seq-Hp5u1N1hjpyS6Ycq0ChF>, <https://benchling.com/s/seq-rW8bte6rTRsuCXbU3L4m>, and <https://benchling.com/s/seq-Orjq9I7OVr1ttUA4Qhzg>, respectively.

Expression of *ObPPT-1* and *ObPPT-2* in *P. pastoris*. *P. pastoris* yeast strains SOB03–05 were cultivated in YPD media with shaking in 15 mL culture tubes and then inoculated into 500 mL shake flasks with 100 mL of BMGY medium at 30 °C to $\text{OD}_{600} = 2\text{--}6$. The cells were collected by centrifugation and resuspended in BMMY medium. Then, the resuspended cells were incubated at 30 °C for 120 h, with the addition of 0.5% MeOH every 24 h.

Metabolite Extraction and GC-MS Analysis. The supernatant of the fermentation was collected from 100 mL of culture by centrifugation and extracted three times with 100 mL of EtOAc. EtOAc extracts were combined and concentrated to afford an organic extract. And then the extract was dissolved with 1.5 mL of CHCl_3 and analyzed using an Agilent 7890 GC-5975 MS instrument under electronic impact at 70 eV. The oven temperature was initially set at 70 °C, raised from 70 to 130 °C (5 °C min^{-1}), then elevated from 130 to 180 °C (10 °C min^{-1}), and then elevated from 180 to 300 °C (5 °C min^{-1}).

■ ASSOCIATED CONTENT

Supporting Information

The Supporting Information is available free of charge at <https://pubs.acs.org/doi/10.1021/acs.jnatprod.0c01101>.

Complete description of methods, additional tables, and figures, including structure elucidation and NMR spectra for compounds 1–12 (PDF)

■ AUTHOR INFORMATION

Corresponding Authors

Jiang-Miao Hu — State Key Laboratory of Phytochemistry and Plant Resources in West China and Yunnan Key Laboratory of Natural Medicinal Chemistry, Kunming Institute of Botany, Chinese Academy of Sciences, Kunming 650201, People's Republic of China; orcid.org/0000-0002-9013-8489; Email: hujiangmiao@mail.kib.ac.cn

Jun Zhou — State Key Laboratory of Phytochemistry and Plant Resources in West China and Yunnan Key Laboratory of Natural Medicinal Chemistry, Kunming Institute of Botany, Chinese Academy of Sciences, Kunming 650201, People's Republic of China; Email: jzhou@mail.kib.ac.cn

Authors

Fu-Cai Ren — State Key Laboratory of Phytochemistry and Plant Resources in West China and Yunnan Key Laboratory of Natural Medicinal Chemistry, Kunming Institute of Botany, Chinese Academy of Sciences, Kunming 650201, People's Republic of China; University of Chinese Academy of Sciences, Beijing 100049, People's Republic of China

Li Liu — State Key Laboratory of Phytochemistry and Plant Resources in West China and Yunnan Key Laboratory of Natural Medicinal Chemistry, Kunming Institute of Botany, Chinese Academy of Sciences, Kunming 650201, People's Republic of China; University of Chinese Academy of Sciences, Beijing 100049, People's Republic of China

Yong-Feng Lv — State Key Laboratory of Phytochemistry and Plant Resources in West China and Yunnan Key Laboratory of Natural Medicinal Chemistry, Kunming Institute of Botany, Chinese Academy of Sciences, Kunming 650201, People's Republic of China; University of Chinese Academy of Sciences, Beijing 100049, People's Republic of China

Xue Bai — State Key Laboratory of Phytochemistry and Plant Resources in West China and Yunnan Key Laboratory of Natural Medicinal Chemistry, Kunming Institute of Botany, Chinese Academy of Sciences, Kunming 650201, People's Republic of China

Qian-Jin Kang – State Key Laboratory of Microbial Metabolism, Joint International Research Laboratory of Metabolic & Developmental Sciences, and School of Life Sciences & Biotechnology, Shanghai Jiao Tong University, Shanghai 200240, People's Republic of China

Xiao-Jing Hu – State Key Laboratory of Microbial Metabolism, Joint International Research Laboratory of Metabolic & Developmental Sciences, and School of Life Sciences & Biotechnology, Shanghai Jiao Tong University, Shanghai 200240, People's Republic of China

Hong-Dan Zhuang – State Key Laboratory of Phytochemistry and Plant Resources in West China and Yunnan Key Laboratory of Natural Medicinal Chemistry, Kunming Institute of Botany, Chinese Academy of Sciences, Kunming 650201, People's Republic of China

Liu Yang – State Key Laboratory of Phytochemistry and Plant Resources in West China and Yunnan Key Laboratory of Natural Medicinal Chemistry, Kunming Institute of Botany, Chinese Academy of Sciences, Kunming 650201, People's Republic of China

Complete contact information is available at:

<https://pubs.acs.org/10.1021/acs.jnatprod.0c01101>

Notes

The authors declare no competing financial interest.

ACKNOWLEDGMENTS

This work was financially supported by the National Key Research and Development Program of China (2017YFD0201402) and Yunnan Provincial Science and Technology Department (No. 2017ZF003-04).

REFERENCES

- (1) Barron, D.; Ibrahim, R. K. *Phytochemistry* **1996**, *43*, 921–982.
- (2) Sasaki, K.; Mito, K.; Ohara, K.; Yamamoto, H.; Yazaki, K. *Plant Physiol.* **2008**, *146*, 1075–1084.
- (3) Mukai, R. *Biosci., Biotechnol., Biochem.* **2018**, *82*, 207–215.
- (4) Saleh, O.; Haagen, Y.; Seeger, K.; Heide, L. *Phytochemistry* **2009**, *70*, 1728–1738.
- (5) Heide, L. *Curr. Opin. Chem. Biol.* **2009**, *13*, 171–179.
- (6) Orjala, J.; Erdelmeier, C. A. J.; Wright, A. D.; Rali, T.; Sticher, O. *Planta Med.* **1993**, *59*, 546–551.
- (7) Hirota, M.; Miyazaki, S.; Minakuchi, T.; Takagi, T.; Shibata, H. *Biosci., Biotechnol., Biochem.* **2002**, *66*, 655–659.
- (8) Flores, N.; Jimenez, I. A.; Gimenez, A.; Ruiz, G.; Gutierrez, D.; Bourdy, G.; Bazzocchi, I. L. *J. Nat. Prod.* **2008**, *71*, 1538–1543.
- (9) Editorial Committee of Flora of China. *Flora of China* **1999**, *18*, 123–126.
- (10) Fukuoka, M. *Chem. Pharm. Bull.* **1982**, *30*, 3219–3224.
- (11) Saijo, R.; Nonaka, G.; Nishioka, I. *Phytochemistry* **1990**, *29*, 267–270.
- (12) Kuo, W. L.; Huang, Y. L.; Shen, C. C.; Shieh, B. J.; Chen, C. C. *J. Chin. Chem. Soc.* **2007**, *54*, 1359–1362.
- (13) Orjala, J.; Erdelmeier, C. A. J.; Wright, A. D.; Rali, T.; Sticher, O. *Phytochemistry* **1993**, *34*, 813–818.
- (14) Winkelblech, J.; Fan, A. L.; Li, S. M. *Appl. Microbiol. Biotechnol.* **2015**, *99*, 7379–7397.
- (15) Van Lanen, S. G.; Lin, S.; Shen, B. *Proc. Natl. Acad. Sci. U. S. A.* **2008**, *105*, 494–499.
- (16) Okada, K.; Ohara, K.; Yazaki, K.; Nozaki, K.; Uchida, N.; Kawamukai, M.; Nojiri, H.; Yamane, H. *Plant Mol. Biol.* **2004**, *55*, 567–577.
- (17) Yang, Y.; Fu, L.; Zhang, J.; Hu, L.; Xu, M.; Xu, J. *PLoS One* **2014**, *9*, No. e99537.

(18) Geisse, S.; Gram, H.; Kleuser, B.; Kocher, H. P. *Protein Expression Purif.* **1996**, *8*, 271–282.

(19) Dai, Z.; Liu, Y.; Zhang, X.; Shi, M.; Wang, B.; Wang, D.; Huang, L.; Zhang, X. *Metab. Eng.* **2013**, *20*, 146–156.

(20) Ro, D. K.; Paradise, E. M.; Ouellet, M.; Fisher, K. J.; Newman, K. L.; Ndungu, J. M.; Ho, K. A.; Eachus, R. A.; Ham, T. S.; Kirby, J.; Chang, M. C. Y.; Withers, S. T.; Shiba, Y.; Sarpong, R.; Keasling, J. D. *Nature* **2006**, *440*, 940–943.

(21) Ryu, M.; Kim, M.; Jeong, M.; Jang, J.; Lee, M.; Jin, H. E.; Jung, J. W. *Synth. Commun.* **2017**, *47*, 818–824.

(22) Monks, A.; Scudiero, D.; Skehan, P.; Shoemaker, R.; Paull, K.; Vistica, D.; Hose, C.; Langley, J.; Cronise, P.; Vaigrowloff, A.; Graygoodrich, M.; Campbell, H.; Mayo, J.; Boyd, M. *J. Natl. Cancer Inst.* **1991**, *83*, 757–766.

(23) Saitou, N.; Nei, M. *Mol. Biol. Evol.* **1987**, *4*, 406–425.